

# Numerical Assessment of the Influence of End Conditions on Constitutive Behavior of Geomaterials

Boris Jeremić<sup>\*</sup> and Zhaohui Yang<sup>†</sup> and Stein Sture<sup>‡</sup>

16. August, 2004

*published in the ASCE Journal of Engineering Mechanics, Volume 130, issue 6, June  
2004*

## Abstract

In this paper we investigate the behavior of elastic–plastic specimens during testing in a triaxial apparatus. In particular, an investigation of the influence of a number of imperfections on the observed behavior of a specimen is performed. To this end, we present influences of end platen friction, end platen inclinations and the shape of specimen on what we broadly understand by ”constitutive behavior”. We investigate the issues related to the constitutive as opposed to boundary value behavior or elastic plastic specimens. We present a number of examples to illustrate the differences between different types of response, which are usually, and wrongly, just called the constitutive behavior.

## 1 Introduction

It has been long argued that the constitutive behavior of engineering materials cannot be accurately deduced from standard laboratory experiments [6]. Laboratory testing of a specimen is intended to represent a single point in a material

---

<sup>1</sup>Department of Civil and Environmental Engineering, University of California, One Shields Ave., Davis, CA 95616, Member ASCE, Email: [Jeremic@ucdavis.edu](mailto:Jeremic@ucdavis.edu).

<sup>2</sup>Civil Engineering Department, University of Alaska Anchorage, Anchorage, AK 99508, Associate Member ASCE.

<sup>3</sup>Department of Civil, Environmental, and Architectural Engineering, University of Colorado, Boulder, CO 80309-0428, U.S.A. Member ASCE.

continuum, thus allowing for constitutive behavior to be deduced. The validity of this assumption depends on the achieved uniformity of stress and strain fields within a specimen. The uniformity depends to a large extent on the configuration of the specimen (including initial non-uniformity and boundary conditions), type of the loading control (force or displacement, fast or slow...) and the measurement of stresses and strains at the specimen surface. In respect to the influence of boundary conditions, it is important to recognize that St. Venant principle<sup>1</sup> states that the stress distribution over cross sections (within a specimen in this case) is uniform only if the external forces applied at the ends are distributed over the end section in the same manner as they are supposed to be inside the specimen.

A number of Authors have been investigating the influence of boundaries on results of laboratory experiments. In particular a number of finite element, analytical and photoelastic studies have been performed, as summarized by [6]. More specifically, the non-uniformities of the stress distribution within the specimen are primarily due to the effects of the friction between end platens and the specimen. The issue of the influence of end platens on test results has been researched for more than 100 years. An elastic solution was worked out by [2] for a cylindrical specimen with parallel (horizontal) end platens and an assumptions of complete friction between end platens and the specimen. Almost half a century later, [5] used Fourier series to solve the elastic problem. The solution was quite tedious as he had to perform hand computations and use graphical techniques.

In what follows we use finite element simulations to investigate the influence of various end platen condition to the constitutive behavior of the specimen.

## 2 Material Model Description

In this section we briefly describe material model used in our numerical experiments. It should be noted that the elastic-plastic formulation and implementation follows closely our recent work [4].

A simple material model was used for this numerical study. The idea behind such a simple model is to actually show that even the very simple model can display a spectrum of different results depending on the actual experimental

---

<sup>1</sup>See [7] and references therein.

setup. The elastic plastic specimen used in this study was simulated using a elastic–perfectly plastic Drucker–Prager material model with non-associated flow rule. The Young’s modulus varies with confining pressure similarly to the work by [3] and [1]), as shown in Eqn. (1).

$$E = E_o \left( \frac{p}{p_a} \right)^a \quad (1)$$

where  $E_o$  is Young’s Modulus at atmospheric pressure,  $p$  is the effective mean normal stresses,  $p_a$  is the atmospheric pressure, and  $a$  is constant for a given void ratio ( $a = 0.5$  was used in this work). The following parameters were used for the specimen (medium dense sand): friction angle  $\phi$  of  $37^\circ$ , a  $0^\circ$  dilation angle,  $E_o = 17400$  kPa, Poisson’s ratio of 0.35 and unit weight of  $14.50$  kN/ $m^3$ .

### 3 Numerical Examples

A series of numerical simulations of triaxial shearing on dry sand specimens has been carried out elongated specimens to investigate the effects of imperfections on the constitutive behavior of soils. The end conditions studied include various frictions and inclinations of end platens. This section presents the simulation results, including deviatoric stress– axial strain ( $q - \epsilon_q$ ) behavior, plastic zone propagation, and elastic zone. Without exception, a confining pressure of 100 kPa were applied on all specimens before axial loading. It is noted that the deviatoric stress  $q$  is defined as  $(\sigma_1 - \sigma_3)$ , which is averaged over all elements and numerical integration points. The axial strain  $\epsilon_q$  is computed by normalizing the displacement of top end platen with the original height of the sample.

Triaxial specimens for soils have a typical length to diameter ratio of 2.0 to 2.5. In this study, a prismatic specimen with a length to width ratio of 2.0 ( called elongated specimen or 2 to 1 specimen in the rest of the paper) was meshed with  $10 \times 10 \times 20$  elements and analyzed with different end conditions, including level end platens, inclined end platens, and level end platens with friction layer between platen and specimen.

#### 3.1 Level End–Platens

Figure 1 shows the  $q - \epsilon_q$  responses of the elongated specimen using fixed (sticking, complete friction) end platens and free of friction platens. The effects of

end friction are not as pronounced as there is enough length within a specimen to develop somewhat uniform stress and strain field.

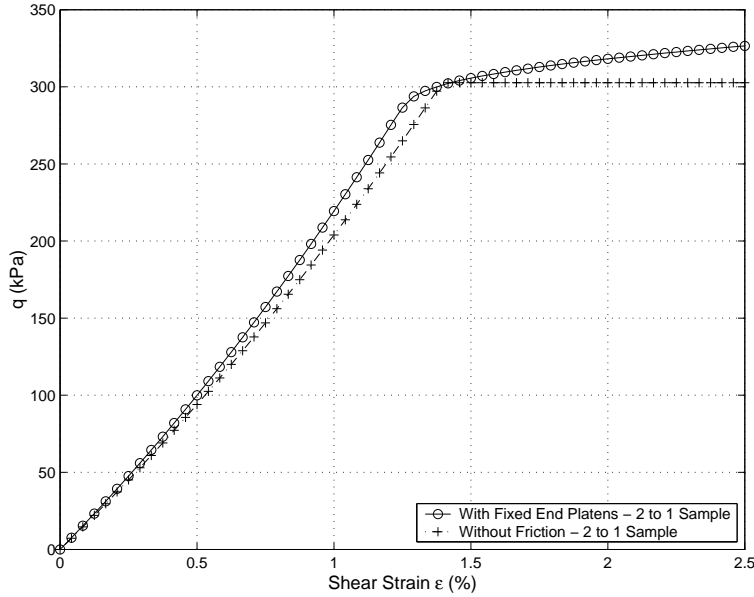


Figure 1: The influence of end friction on deviatoric stress versus axial strain responses of elongated specimen.

A plastic zone propagation for elongated specimen is animated in Figure 2. It is worthwhile to note that the strain values corresponding to each snapshot are increasing from 0 to 3.0% in Figures 2, 5 and 7. From Figure 2 it is obvious that plastic zone has enough length to be fully established within the central zone of the specimen. It is interesting to note that the elastic zone close to the specimen ends remains sizable.

### 3.2 Inclined End-Platens

It is believed that the very minor inclination of end platens can also cause significant non-uniformities in stress distribution, and therefore affect the constitutive behavior. To investigate the effects of end platen inclination, the same mesh as above was analyzed with inclined top platen, which was simulated by applying inclined displacement increments to the top platen. The inclination angle linearly increases (starting from zero) during loading. Therefore, the inclination

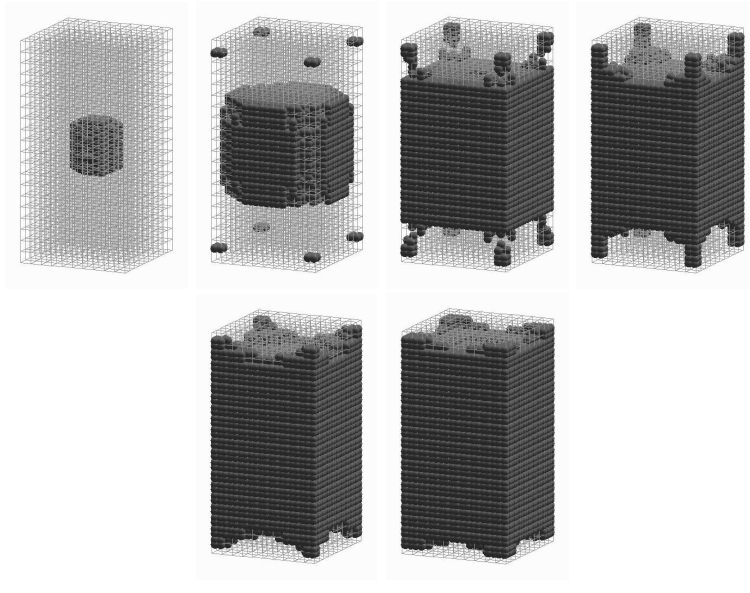


Figure 2: Deformed elongated specimen propagation of plastic zone for a simulation using  $10 \times 10 \times 20$  mesh with fixed level end platens.

angle at the end of loading, i.e. the maximum inclination angle, was used to identify each case.

A number of simulations with various maximum inclination angles, i.e.  $0.54^\circ$ ,  $0.89^\circ$ ,  $2.34^\circ$ ,  $2.95^\circ$ , and  $3.31^\circ$ , were conducted and the  $q - \epsilon_q$  responses were shown in Figure 3. For comparison, the responses with no end friction and with fixed end platen conditions with parallel top platen were also plotted in the same Figure. As can be seen from Figure 3, the  $q - \epsilon_q$  response at very small max. inclination angle of  $0.54^\circ$  is weaker and specimen yields earlier than that with parallel end platens. However, the response becomes significantly weaker as the max. inclination angle increases from  $0.54^\circ$  to  $3.31^\circ$ . For example, at 2% of axial strain, deviatoric stress decreases from 312 kPa to 252 kPa, about 20%, as max. inclination angle increases from  $0.54^\circ$  to  $3.31^\circ$ .

To further quantify the weakening effect of inclined end platens, the mobilized friction angle  $\phi_{mob}$  at 2% of axial strain was computed according to Eqn. 2 and plotted in Figure 4 against maximum end platen inclination angle.

$$\eta = \frac{6 \sin \phi_{mob}}{3 - \sin \phi_{mob}} \quad (2)$$

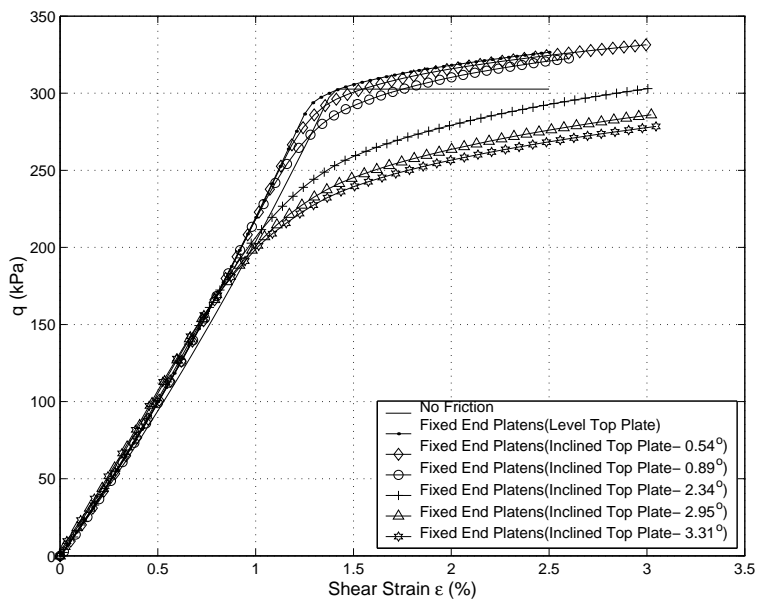


Figure 3: Comparison of the deviatoric stress versus axial strain response for an elongated specimen without friction, with friction (parallel end platens) and variations (small) of inclinations including end platens friction.

where  $\eta$  is defined as  $q/p$ ,  $p$  is the effective mean normal stresses. It can be seen from Figure 4 that as inclination angle increases from  $0^\circ$  to  $3.31^\circ$ , the mobilized friction angle drops from  $37.9^\circ$  to  $34.2^\circ$ . The actual friction angle of sand specimen used for computations is  $\phi = 37^\circ$ .

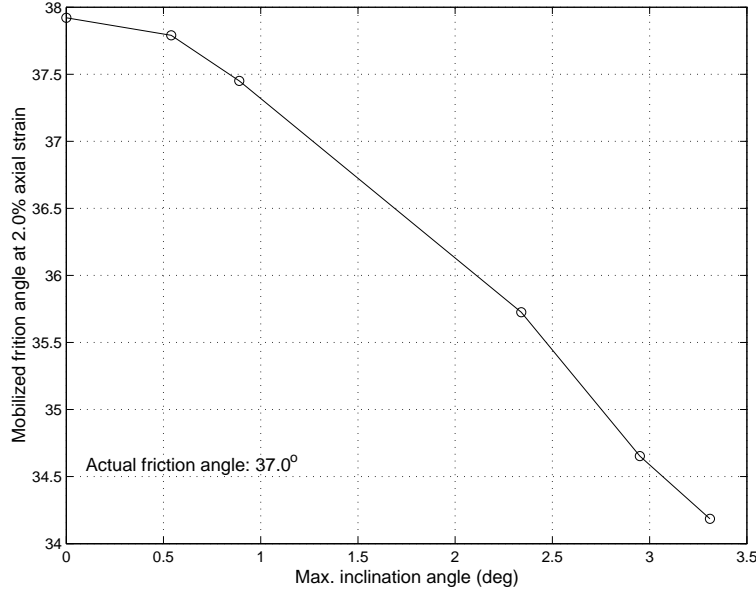


Figure 4: Comparison of the mobilized friction angle at 2% axial strain for various max. inclinations of end platens. Actual material friction angle is  $37^\circ$ .

As mentioned before, the inclination of end platen effects are caused by the significant non-uniformities in the stress field induced by inclined end platens, as demonstrated in Figure 5, which shows the deformed elongated specimen and propagation of plastic zone during loading by inclined end platens with a max. inclination angle of  $2.34^\circ$ . Comparison of Figure 5 and 2 shows there is a great difference in the propagation of plastic zone between parallel and inclined end platen loadings. The specimen is distorted sideways rather than bulging uniformly. It is also worth mentioning that the elastic zone zone remains significantly larger than in the level end platen case, however the distribution is rather non-uniform, and the elastic zone is confined to two opposite corners of the specimen.

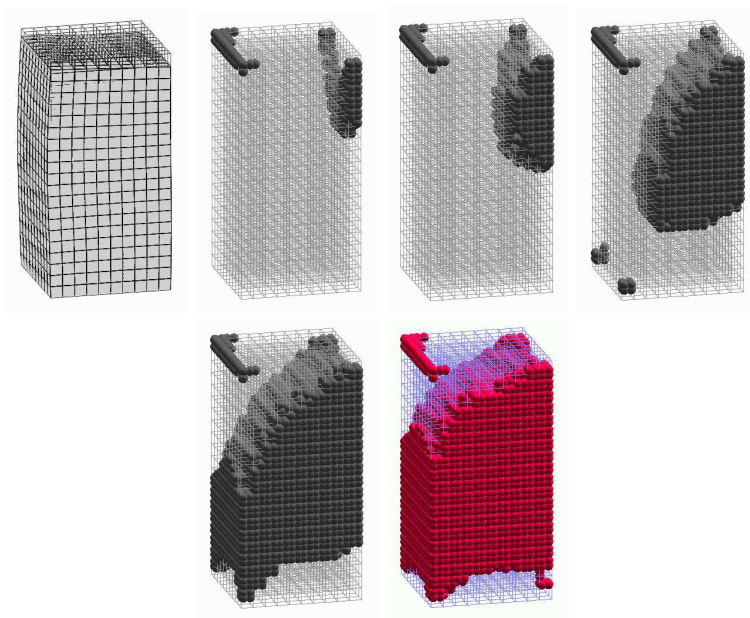


Figure 5: Deformed elongated specimen and a propagation of plastic zone for a specimen with friction and inclined end platens.



### 3.3 Level End-Platens with a Friction Layer Between Platen and Specimen

In the aforementioned simulation, only two extreme ends of friction conditions, i.e. free of friction and fixed end platens, were investigated. An investigation of the effects of different friction angles at end platens on the so called constitutive behavior of the specimen. Special friction layers between end platen and specimen were designed to study the effects of end friction quantitatively. These friction layers were also modeled by Drucker-Prager model with non-associated flow rule (certain friction angle and dilation angle of  $0^\circ$ ).

Three cases with different friction angles, i.e.  $\phi = 5^\circ, 10^\circ$ , and  $15^\circ$  were simulated and the  $q - \epsilon_q$  responses were plotted in Figure 6. Also shown in Figure 6 were the  $q - \epsilon_q$  responses for no friction case ( $\phi = 0^\circ$ ) and fixed (sticking) end platens case. The fixed end platen case can be interpreted to have a friction layer with  $\phi = 37^\circ$  while the actual interface has  $\phi = 90^\circ$ . It can be seen that as the end platen friction decreases, the response after yielding is becoming flatter and closer to the specimen's expected constitutive behavior.

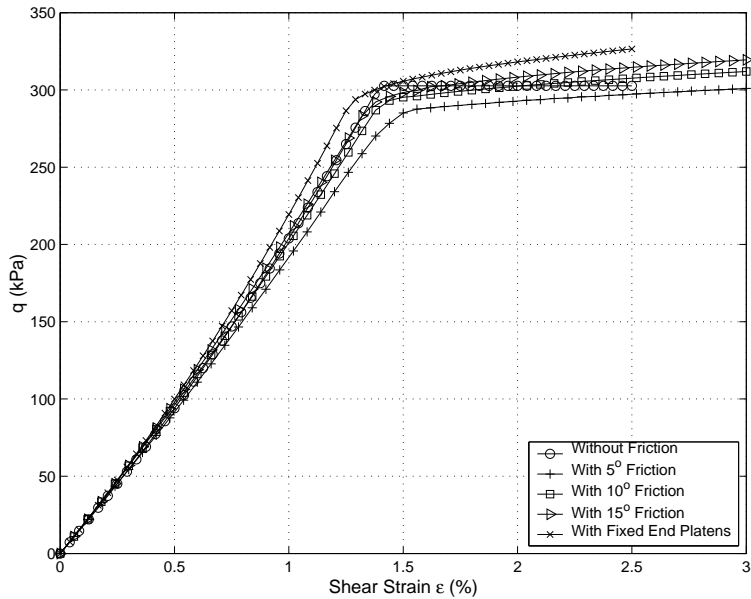


Figure 6: Comparison of the response for various end friction angles.

Figure 7 shows the plastic zone propagation for model with friction layers of  $5^\circ$  at its ends. The propagation of plastic zone in this case is very interesting. First the friction layers yield at their edges due to end friction, and then the plastic zone extends to the two weak layers at the ends. After that, the elements close to weak friction layers start to plastify and the plastic zone forms a cone shape and propagates into the middle of specimen and finally spreads to most of the elements in the specimen. Among all the plastic zone propagation plots (elongated specimen loaded by inclined end platens, elongated specimen loaded by parallel end platens with different end friction), this end condition allows the soil elements to yield most uniformly. It is also interesting to compare this yielding propagation (shown in Figure 7) with that of a fully fixed end platen shown in Figure 2. The difference is explained by the fact that for the specimen from Figure 7 there is a lacking confinement at the specimen ends, so it yields first at the ends, and then the yield propagates throughout the specimen. On the other hand specimen from Figure 2 is restrained, confined at the ends, and therefor the yielding is forced far away from the confined zone, into the specimen center.

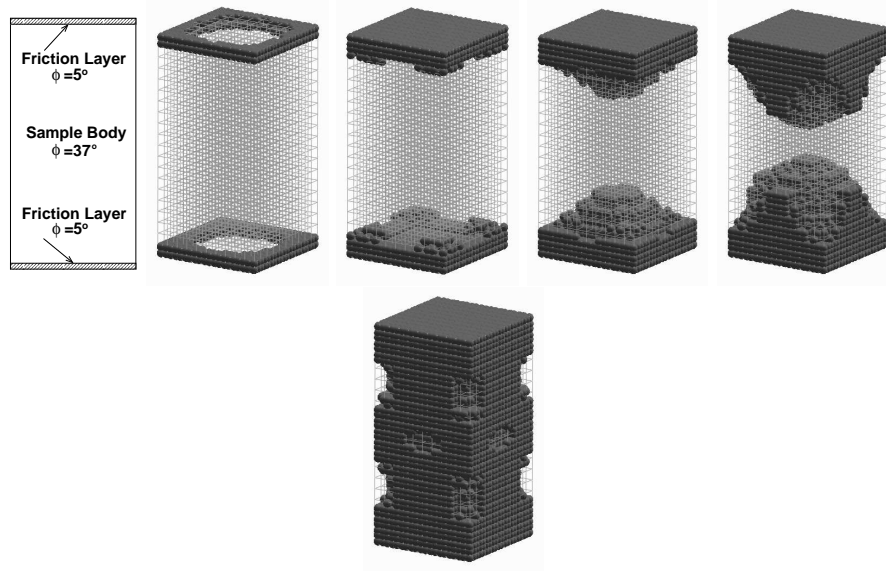


Figure 7: Sketch of sample with friction layers and a propagation of plastic zone for a specimen with  $5^\circ$  friction and level top end platen.

The interesting observation is that even-though it seems like all of the specimen has yielded (see last of Figures 7), the response is still hardening. Figure 8 shows the remaining elastic zone within specimen at the end of loading (at the 2.2% axial strain) for various end platen friction angles. As can be seen, the elastic zone corresponding to end friction of  $5^\circ$  is the smallest, which also suggests the most uniform stress field in the specimen.

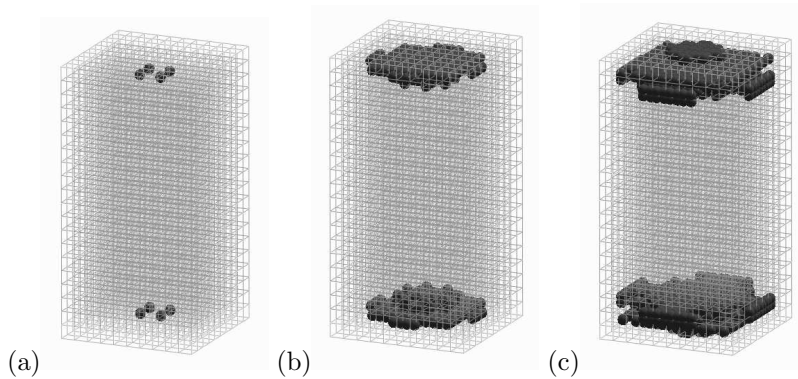


Figure 8: The elastic zone at 2.2% axial strain for specimens with different end friction: (a)  $5^\circ$  (b)  $10^\circ$  and (c)  $15^\circ$ .

## 4 SUMMARY

In this paper an investigation of the behavior of elastic–plastic specimens during testing under triaxial stress conditions was presented. The influence of a number of imperfections on the assumed constitutive behavior of specimens was assessed and illustrated with number of examples. The work presented here is part of our endeavor to understand the ”real” behavior of geomaterials.

## Acknowledgment

This work was supported in part by the Earthquake Engineering Research Centers Program of the National Science Foundation under Award Number EEC-9701568.

## References

- [1] DUNCAN, J. M., AND CHANG, C.-Y. Nonlinear analysis of stress and strain in soils. *Journal of Soil Mechanics and Foundations Division* 96 (1970), 1629–1653.
- [2] FILON, L. N. G. The elastic equilibrium of circular cylinders under certain practical systems of load. *Philosophical Transactions of the Royal Society of London* 198, Series A (1902).
- [3] JANBU, N. Soil compressibility as determined by odometer and triaxial tests. In *Proceedings of European Conference on Soil Mechanics and Foundation Engineering* (1963), pp. 19–25.
- [4] JEREMIĆ, B., AND YANG, Z. Template elastic–plastic computations in geomechanics. *International Journal for Numerical and Analytical Methods in Geomechanics* 26, 14 (2002), 1407–1427. available as CGM report at: <http://sokocalo.engr.ucdavis.edu/~jeremic/publications/CGM0102.pdf>.
- [5] PICKETT, G. Application of the fourrier method to the solution of certain boundary problems in the theory of elasticity. *Journal of Applied Mechanics* 2 (1944).
- [6] SAADA, A. S., AND TOWNSEND, F. C. Strength laboratory testing of soils. *ASTM STP 740* (June 25th 1981), 7–77. A State of the Art paper presented at the ASTM Symposium on the Shear Strength of Soils, June 25, 1980,.
- [7] TIMOSHENKO, S. S. *History of Strength of Materials*. McGraw–Hill, Book Company, Inc., 1953.